1999

Gamut Mapping for Pictorial Images

Gustav Braun
Rochester Institute of Technology

Mark Fairchild
Rochester Institute of Technology

Gamut Mapping for Pictorial Images

Gustav J. Braun and Mark D. Fairchild*

Keywords: Color Gamut Mapping, Contrast, Image Processing

Abstract: A psychophysical evaluation was performed to test the quality of several color gamut mapping algorithms. The task was to determine which mapping strategy produced the best matches to the original image. Observer preference was not considered. The algorithms consisted of both device-dependent and image-dependent mappings. Three types of lightness scaling functions (linear compression, chroma weighted linear compression, and image-dependent sigmoidal compression) and four types of chromatic mapping functions were tested (linear compression, knee-point compression, "sigmoid-like" compression, and clipping). The source and destination devices considered were a monitor and a plain-paper inkjet printer respectively. The results showed that, for all of the images tested, the algorithms that used image-dependent sigmoidal lightness remapping functions produced superior matches to those that utilized linear lightness scaling. In addition, the results support using chromatic compression functions that were closely related to chromatic clipping functions.

Introduction

Color gamut mapping is an integral part of digital color reproduction. The need for color gamut mapping arises when the source image contains color values that are not physically realizable on the destination device. This situation frequently arises in cross-media color reproduction when the two imaging systems utilize different primary sets. One of the most notable examples of this is when a monitor original is reproduced lithographically. In general, the color gamut of the monitor is larger than the lithographic print. Thus, some type of mapping must be utilized to move the out-of-gamut monitor (source) pixels into the gamut of the lithographic (destination) gamut.

Throughout this article, the gamut mismatch between two devices will be characterized into lightness and chromatic components. A lightness mismatch exists between two gamuts when their respective black-point lightnesses are not equal. This results in a difference in the lightness dynamic range of the devices

* Munsell Color Science Laboratory
Center for Imaging Science
Rochester Institute of Technology
Rochester, New York

(i.e., the device with the lower black-point lightness has the larger lightness dynamic range). The chromatic components of a gamut mismatch result from the hue, lightness, and chroma differences of the primaries. Additional factors such as media characteristics (e.g., paper gloss, paper "whiteness", fluorescence) and digital processing (e.g., halftoning and UCR/GCR) effect the gamut of an imaging device.

When designing a color gamut mapping strategy, several factors need to be considered. Ultimately, the reproduction task needs to be considered. For example, reproduction of a business graphic image may place more emphasis on the chromatic image content and the smoothness of subtle lightness and chroma gradients. Less emphasis may be placed on the lightness and hue of the reproduction. For pictorial image gamut mapping tasks, preservation of the lightness contrast and the hue of the original may be the most important.

The goal of this study was to test the effectiveness of using image-dependent contrast preserving lightness rescaling functions along with image-dependent non-linear chromatic compression functions. The context under which these experiments were performed was to determine which algorithm produced the reproductions that were the best match to the original. The following sections detail the motivation and the form of the gamut mapping algorithms used, the psychophysical experiments performed, and conclusions.

Gamut Mapping Algorithms

Lightness scaling

In color gamut mapping for pictorial images, one of the biggest obstacles that needs to be overcome is the lightness dynamic range differences between the source and destination gamuts. Typically, linear lightness rescaling functions have been used to scale the input image data into the gamut of the destination device (Stone and Wallace (1991), Viggiano and Wang (1992), MacDonald and Morovic (1995), Montag and Fairchild (1997), Morovic and Luo (1997, 1998), Morovic (1998)), as shown in Figure 1a. The linear lightness remapping process suffers from a global reduction in the perceived lightness contrast and an increase in the mean lightness of the remapped image. When the dynamic range difference between the source and destination devices is significant, output images tend to appear light and often times contain a "milky" or "hazy" appearance in the shadow detail.

When the dynamic range differences between the input and output gamuts are small, "hard" clipping might be considered, as shown in Figure 1a. In this case, all of the input image pixels whose lightness are less than that of the destination black-point are simply clipped to that value. This process has the advantage of preserving the lightness of most of the image. However, when the source and

destination black-points are significantly different, the many-to-one mapping associated with clipping can result in “flat” or “blocked” shadowed regions.

In order to overcome the limitations of the contrast loss associated with linear lightness mapping and the texture loss associated with “hard” clipping, Braun and Fairchild (1999) have developed an adaptive lightness rescaling process that utilizes sigmoidal mapping functions. The form of the sigmoidal functions was based on a cumulative normal function. They are adaptive in that their shape is derived from the lightness histogram of the input image and depends on the black-point differences between the source and destination gamuts. Example remapping functions are shown for three different histogram shapes in Figure 1b. The shape of the sigmoidal remapping function aids in the dynamic range mapping process in two ways: 1.) By increasing the image contrast during the remapping process, the perceived lightness contrast of the original is approximately maintained across a wide range of destination dynamic ranges. 2.) The low end compression is gradual, thus reducing the low-end textural defects of hard-clipping.

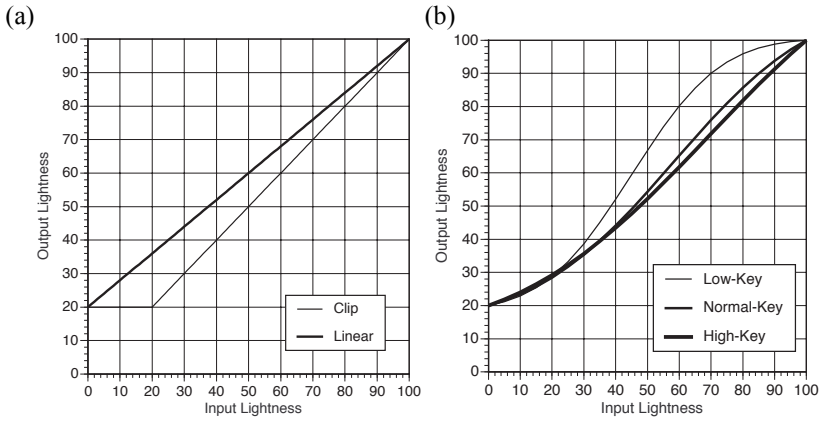

Figure 1a,b. Lightness rescaling functions used for rescaling from an input dynamic range of 0-100 lightness units to an output range of 20-100 lightness units. (a) Device-dependent clipping and linear compression functions. (b) Image-dependent sigmoidal contrast preserving remapping functions for three image lightness keys (Braun and Fairchild (1999)).

Chroma mapping functions

Chromatic remapping functions can be broken down into scaling and clipping functions. Scaling functions act on all pixels in the image. Clipping functions only act on the out-of-gamut pixels in the image. In a gamut mapping task where the lightness and the chromatic channels are mapped sequentially, typically the

lightness channel is mapped first and the chromatic channels are mapped second. The most common forms of chromatic scaling functions are linear and knee-functions (Gentile, Walowitt, and Allebach (1991)), shown in Figure 2. The linear compression function globally reduces the chromatic signal throughout the entire gamut. The knee-function rescalings preserve the chromatic signal through the central portion of the gamut while compressing the chromatic signal near the edges of the gamut. This has the effect of preserving the character of the low chromatic signal, where color shifts are very noticeable, and performing the majority of the chromatic compression where the differences are less noticeable.

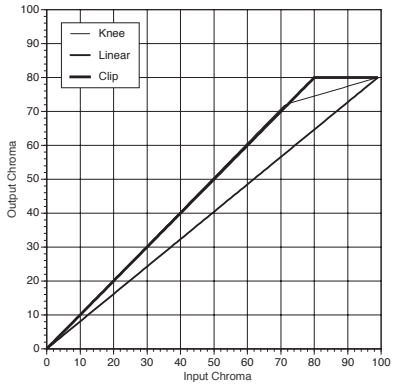

Figure 2. Illustration of three chroma mapping functions. The examples shows and input chroma range from 0-100 units mapped into an output range of 0-80 units. The knee point of the two-piece linear knee function was set at 90 percent of the maximum output chroma.

As with lightness remapping, the chromatic clipping algorithms have the advantage that they leave the majority of the chromatic content unchanged in the mapping process. However, just as with lightness clipping the many-to-one process of chromatic clipping can have artifacts when a group of spatially related pixels gets mapped to the same point in color space. The use of scaling functions reduces these effects. In general, non-linear chromatic compression functions like knee-functions perform better than linear or clipping as the range of chromatic compression increases. Using these types of functions helps to maintain the chromatic contrast of the original scene while avoiding clipping artifacts.

A “sigmoid-like” chromatic remapping function was introduced based on the success of the sigmoidal lightness remapping function in maintaining the lightness contrast of the original scene in the reduced dynamic range of the destination device. The form of this scaling function is given in Figure 3. The

desired effect with using this type of rescaling function was to increase the chromatic image contrast so that the perceived chromatic contrast would be better maintained under the reduced range conditions of the destination device.

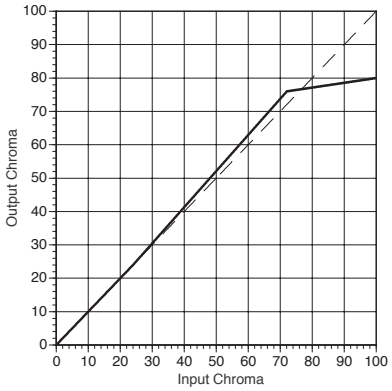

Figure 3. "Sigmoid-like" chroma scaling function. This function has three linear segments. The first segment is a 1-to-1 mapping (slope=1.0). The second segment expands the input chroma, slope >1.0. The third segment (slope < 1.0) compresses the high-end chroma values into the destination gamut.

Chroma scaling directions

Many researchers have looked at the optimal direction to scale for different gamut mapping tasks (MacDonald and Morovic (1995), Katoh and Ito (1996), Morovic and Luo (1997), Ebner and Fairchild (1998a)). Of these studies, the work by Morovic and Luo was conducted predominantly for pictorial images. Their conclusion was that the cusp point of the destination gamut was the most robust point toward which to scale. In their studies, they preserved the metric hue angle of the reference color space. They showed that the hue-preserving mapping was as effective as one that rotated the input hue to be more in line with primaries of the destination device (Morovic and Luo (1998)). For the research presented in the current paper, cusp point scaling was utilized due to its general good performance.

Color spaces for gamut mapping

Recently, there have been numerous studies that have shown the need for a uniform color space for gamut mapping (Hung and Berns (1995), Braun, Ebner, and Fairchild (1998), Ebner and Fairchild (1998b), Marcu (1998), McCann (1999)). It has been shown that many of the current color appearance spaces (e.g., Hunt95, CIELAB, CIELUV, CIECAM97s) have significant hue non-linearities (Hung and Berns (1995), Ebner and Fairchild (1998b)). An example

of this can be seen in Figure 4 for CIELAB and CIECAM97s. The implication of these hue non-linearities for color gamut mapping can be dramatic for algorithms that preserve metric hue angle (e.g., h_{ab} in CIELAB). Significant perceived hue shifts can result depending on the amount of lightness and/or chroma compression (Braun, Ebner, and Fairchild (1998)). The most notable example occurs in the "blue" region of color space were a high chroma "blue" is mapped to a lower chroma "purple" when mapped along lines of constant CIELAB metric hue angle.

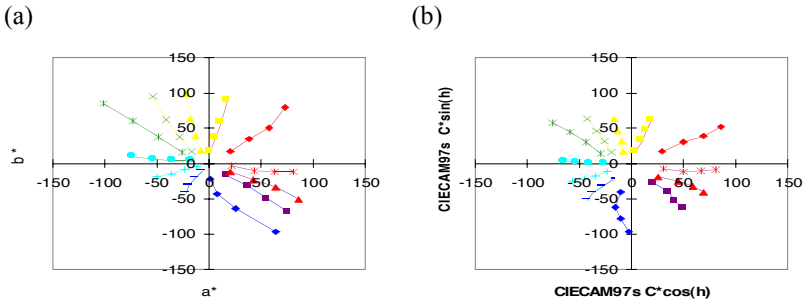

Figure 4a,b. Hung and Berns Lines of constant perceived hue plotted in (a) CIELAB and (b) CIECAM97s.

The color space used for gamut mapping in this study was the Hung and Berns hue-linearized CIELAB color space given by Braun, Ebner, and Fairchild (1998). This color space is identical to CIELAB except in the "blue" region of color space where the perceived hue lines significantly depart from the metric hue angle of CIELAB. Other hue-corrected color spaces developed by Marcu (1998) and McCann (1999) were based on the Munsell data. The advantage of using the Hung and Berns data to correct the CIELAB color space is that their data set extend to much more chromatic colors than the Munsell data. For color gamut mapping this is important since most of the compression happens on high chroma colors where the hue non-linearity is the greatest. An alternate color space would have been to use the IPT color space developed by Ebner and Fairchild (1998b). This space was not selected since it has not yet been fully tested for gamut mapping tasks using pictorial images. However, similar results would be expected.

Device-dependent and image-dependent mappings

Implementation of gamut mapping algorithms that use scaling functions requires that all of the parameters used for the scaling functions be calculated from either the source/destination gamut surface data or from the image/destination gamut surface data. In device-dependent gamut mapping the scaling functions are set by evaluating the differences in the gamut surface data between the source and

destination devices. For image-dependent gamut mapping the scaling functions are set by evaluating the differences between the input image data and the destination gamut. Morovic (1998) has given an excellent description of several device dependent gamut mapping strategies.

Each of these mappings strategies has benefits. The device-dependent mappings can be easily generalized, encoded into multidimensional look-up tables (LUTs), and implemented in color management software (e.g., the ICC paradigm). Image-dependent mappings are less suitable to LUT implementation and are therefore more restrictive in their application in traditional color management software. However, since these gamut mapping algorithms are fine-tuned for each input image, greater flexibility exists for the image-dependent mappings.

Image-dependent mappings can take on many forms. Many researchers have shown the benefit of applying image-dependent mappings to both lightness and chroma scaling functions (Gentile, Walowitt, and Allebach (1991), Montag and Fairchild (1997), Morovic (1998)). For lightness remapping, the image dependence has typically come from scaling the minimum image lightness to the lightness level of the destination device's black-point. In situations where linear lightness scaling is utilized, this can have an impact on the final contrast of the remapped image since less compression is required. Wolski, Allebach, and Bouman (1994) utilized a similar strategy for chroma compression. In their algorithm, they the located the image pixel that had the maximum chroma, for each hue angle. They then used this point to set the chroma scaling so that it would be scaled into a chroma equal to that of the cusp point.

In general, image-dependent mappings can improve the quality of the mapped image over the device-dependent mappings. One of the drawbacks of basing the gamut compression on the lightness of the minimum pixel in the image or the maximum chroma at a given hue angle is that these points could be outliers in the multidimensional image histogram. As such, basing the compression on these points may not be the best possible use of the lightness or chromatic range given the input data set.

An alternate approach is to consider an image gamut that is defined by the form of the multidimensional image histogram. For example, suppose that the three-dimensional histogram of an image was calculated in the CIELAB color space. The volume of CIELAB spanned by this histogram represents the image-gamut. Some of this image-gamut will be contained within the gamut of the destination device. Other portions of the image gamut will be outside the destination gamut. It is possible to base the form of the scaling functions on the differences between the destination device's gamut and the image-gamut. Thus, for the regions were most of the image data is in gamut little compression is needed to move the remaining pixels in gamut. This will result in less overall chromatic compression than the device-gamut approach.

For this study the image-gamut boundary was taken as the 95 percent contour of the cumulative image histogram, calculated in the direction of the chromatic scaling (i.e., the cusp point), Appendix A. The 95 percent contour of the image histogram was used to separate the image-gamut boundary from any outlying image points. Thus, the image-gamut could be considered to contain 95 percent of the pixels of the source image. The philosophy subscribed to was that this boundary contained the most important contextual information about the gamut of the image. The remaining 5 percent of the image data (i.e., outside the image gamut) would not significantly change the appearance of the gamut-mapped image if simply clipped to the gamut surface. Calculation of the image gamut was performed in the Hung and Berns hue-linearized CIELAB LCh color space (Braun, Ebner, and Fairchild 1998).

Experiment

Algorithms Tested

A series of gamut mapping algorithms were generated using the lightness and chroma compression schemes outlined in the previous section. These algorithms were grouped into three lightness rescaling categories (i.e., linear lightness compression (LIN), weighted chroma-dependent linear lightness compression (GCUSP), and image-dependent sigmoidal lightness compression (SIG)) and four chroma scaling categories (i.e., linear cusp-point scaling (LIN), knee-function cusp-point scaling (KNEE), cusp-point clipping (CLP), image-gamut based knee-function scaling (IMGGAM), and "sigmoid-like" cusp-point scaling (ENHANCE)). Using combinations of these lightness and chroma scaling categories, the following six hue-preserving, cusp-point based gamut mapping strategies were used:

1. **LIN_LIN** - Linear lightness compression followed by device-dependent linear chroma compression (Morovic and Luo 1998).

2. **GCUSP** - Weighted, chroma-dependent, linear lightness compression followed by device-dependent linear chroma compression (Morovic and Luo 1998).

3. **SIG_LIN** - Image-dependent sigmoidal lightness compression followed by device-dependent linear chroma compression.

4. **SIG_KNEE** - Image-dependent sigmoidal lightness compression followed by device-dependent knee-function chroma compression. (Note: The knee-point was set at 90 percent of the destination-gamut range).

5. **SIG_CLP** - Image-dependent sigmoidal lightness compression followed by cusp-point clipping.

6. **SIG_ENHANCE** - Image-dependent sigmoidal lightness compression followed by "sigmoid-like" chroma compression.

7. **SIG_IMGGAM** - Image-dependent sigmoidal lightness compression followed by image-gamut based knee-function compression. (Note: The knee-point was set at 90 percent of the destination-gamut range).

Gamut definition

Using the seven algorithms described in the previous section, a gamut mapping psychophysics experiment was performed. In order to avoid the costly task of making hardcopy reproductions and to efficiently utilize a paired-comparison evaluation, this experiment consisted of a simulated print experiment. All of the original images were from the full monitor gamut. These images were gamut mapped into an ink-jet printer gamut. Instead of printing, the CIELAB values of the gamut-mapped images were converted to monitor (RGB) digital counts using a gain-offset-gamma model for the monitor (Berns, Motta, and Gorzynski 1993). These images were displayed with the original on the monitor. Since only gamut compression algorithms were considered, all of the gamut-mapped pixels were within the monitor gamut. In addition, the ink-jet printer essentially fit completely within the monitor gamut, shown in Figure 5 and Figure 6.

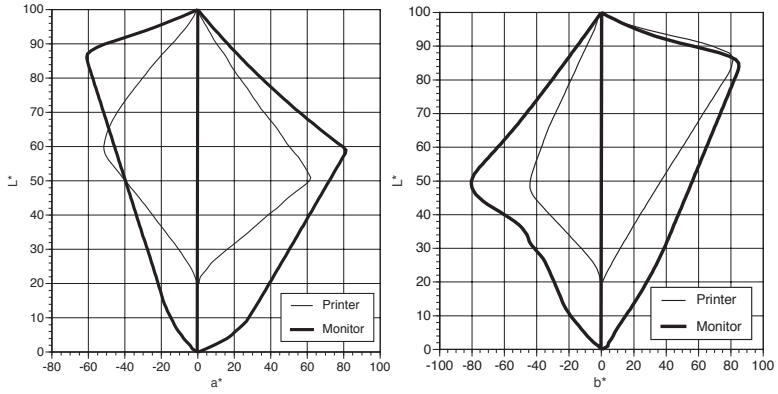

Figure 5. Slices taken through the source (Monitor) and destination (Printer) gamuts along the Hung and Berns hue-linearized CIELAB a* and b* axes.

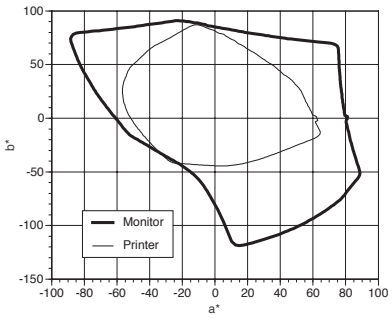

Figure 6. Source (Monitor) and destination (Printer) gamuts projected into the Hung and Berns hue-linearized CIELAB [a*,b*] plane.

For this experiment, all of the images were viewed on a colorimetrically calibrated monitor with white point chromaticities near D65. The monitor was a Sony GDM-2000TC. The source images were converted to CIELAB using a gain-offset-gamma model for the monitor (Berns, Motta, and Gorzynski (1993)). The black-point of the Sony monitor was essentially zero (reproductions were viewed in a dark room). The destination gamut was obtained for a Hewlett Packard HP870Cxi ink-jet printer using plain paper. The black-point of the printer was approximately 18 CIELAB L* units. Both of the gamut surfaces were defined using the process defined by Braun and Fairchild (1997).

Image selection

For this experiment, seven pictorial images were used. These contained a wide variety of scenes and included memory colors such as skin tones and grass. In addition, the features of these images robustly spanned the CIELAB color space. Special attention was given to select images with regions of high chroma red, yellow, green, and blue (all colors that are particularly affected when gamut mapping from monitor to print).

Visual Experiment

The visual experiment consisted of having the twenty observers simultaneously view the original image and pairs of the gamut mapped reproductions. The observers were instructed to select the reproduction that was the closest *match* to the original. They were specifically instructed that the reproduction that was the best match to the original may not be the reproduction that they preferred. Preference will be considered in future experiments.

Results

A series of interval scales, shown in Figure 7, were developed that defined both the rank ordering of the algorithms performance and a gauge of the relative difference between the techniques. These scales were generated using Thurstone's "Law of Comparative Judgments" (Torgerson (1958)). Incomplete matrix calculations were applied due to cases of unanimous agreement between observers which made it impossible to directly calculate the Z-scores for those image pairs. The error bars shown on these plots represent the visual uncertainty between the algorithms. If the mean Z-score of an algorithm is contained within the error bars another algorithm the two algorithms have statistically the same visual performance. The confidence intervals used in the error bar calculations were derived from C = 1.386 / sqrt(N), where N equals the number of observers.

Evaluation of the interval scales indicated that, across the images, the algorithms could be grouped into three significantly different categories. The first category of algorithms was the device-dependent linear lightness and linear chroma compression. This category included the GCUSP_LIN and the LIN_LIN algorithms. For all of the images, these algorithms had much lower scale values than the images mapped using the sigmoidal lightness functions. This was primarily due to their low contrast which resulted from the linear dynamic range mapping.

The second category of results consisted of those images that were mapped using the sigmoidal lightness remapping functions and the linear chroma compression. This gamut mapping strategy created significantly better matches than the first category. This result stresses the importance of faithful reproduction of the lightness contrast of the scene, which is not found with straight linear lightness reproduction.

The third category of algorithms consisted of those that utilized both the sigmoidal lightness remapping functions and the non-linear chroma compression functions (SIG_KNEE, SIG_CLP, SIG_IMGGAM, SIG_ENHANCE). For all of the images, these techniques produced significantly better matches than those produced by the first and second categories of algorithms. There were, however, no significant differences noticed between these four algorithms. These gamut mapping routines resulted in very similar images since the knee-point of the mappings was set at 90 percent of the input gamut range (very similar to cusp-point clipping). The knee-point was set at the 90 percent point of the destination gamut based on the good performance of the clipping algorithms shown by (Montag and Fairchild (1998)) and because of the added flexibility to reduce the possible quantization artifacts of clipping.

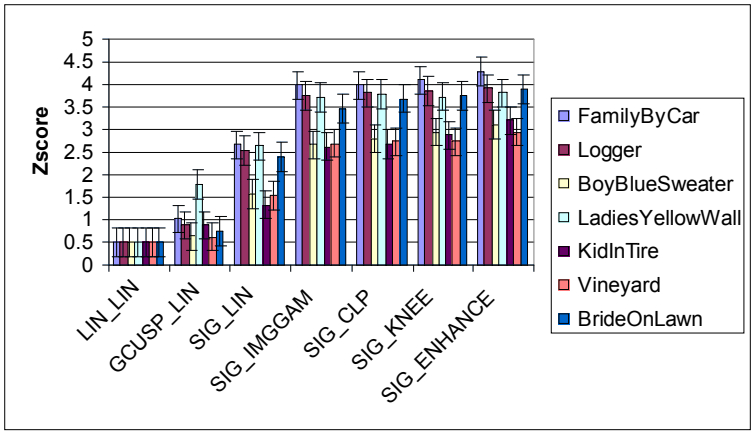

Figure 7. Interval scales for the each image tested. Higher Z-scores inticate that the algorithms produce the better matches. The scale values should only be compared within an image. For example, it is appropriate to compare the difference between the Z-scores for the GCUSP_LIN and SIG_LIN image for the "Logger" image. It would not be appropriate to compare the Z-scores between the "Logger" and the "KidInTire" images for the SIG_CLP algorithm because these images were never compared to each other.

Conclusions

The results of this study indicate that, for color gamut mapping of pictorial images, the biggest factor that affects the match between an original and a reproduction is the lightness contrast rendition. This was shown by the significant improvements obtained using the image-dependent sigmoidal lightness rescaling functions compared to the linear functions. Once the lightness contrast was appropriately mapped, the chromatic compression functions using non-linear knee-functions produced significantly superior reproductions than the linear chromatic compression functions. Little difference was noticed between the chromatic compression functions that were based on the image-gamut and those based on the device-gamut mismatches. Thus, under general conditions it seems reasonable to forgo the complex image-gamut calculations for the chromatic compression when using scaling functions that are very similar to clipping.

Literature Cited

Braun G. J., Ebner F., and Fairchild M. D.
1998 "Color Gamut Mapping in a Hue–Linearized CIELAB Color Space", Proceedings of 6th IS&T/SID Color Imaging Conference, pp. 147–152.

Braun G. J. and Fairchild M. D.
1997 "Techniques for Gamut Surface Definition and Visualization", Proceedings of 5th IS&T/SID Color Imaging Conference, pp. 147–152

Braun G. J. and Fairchild M. D.
1999 "Image Lightness Rescaling Using Sigmoidal Contrast Enhancement Functions", Proceedings of SPIE Electronic Imaging Conference, Vol. 3648, pp. 96-107.

Berns R.S., Motta R.J., and Gorzynski M.E.
1993 "CRT Colorimetry. Part 1: Theory and Practice", Color Research and Applications, Vol. 18, pp. 299-314.

Ebner, F. and Fairchild, M.D.
1998a "Finding Constant Hue Surfaces in Color Space", Proceedings of SPIE, Color Imaging: Device-Independent Color, Color Hardcopy, and Graphic Arts III, Vol. 3300-16, pp.107-117.

1998b "Development and Testing of a Color Space (IPT) with Improved Hue Uniformity", Proceedings of 6th IS&T/SID Color Imaging Conference, pp. 8-13.

Gentile R. S., Walowitt E., and Allebach J. P.
1990 "A comparison of techniques for color gamut mismatch compensation", Journal of Imaging Technology, Vol. 16, pp. 176–181.

Hung P. and Berns R.S.
1995 "Determination of Constant Hue Loci for a CRT Gamut and Their Predictions Using Color Appearance Spaces", Color Research and Application, Vol. 20, No. 5, pp. 285-295.

Katoh N. and Ito M.
1996 "Gamut Mapping for Computer Generated Images (II)", Proceedings of 4th IS&T/SID Color Imaging Conference, pp. 126–129.

MacDonald L. and Morovic J.
1995 "Assessing the Effects of Gamut Compression in the Reproduction of Fine Art Paintings", Proceedings of the 4th IS&T Color Imaging Conference, pp. 194-200.

Marcu G.
1998 "Gamut Mapping in Munsell Constant Hue Sections", Proceedings of the 6th IS&T/SID Color Imaging Conference, pp. 159–162.

McCann J. J.
1999 "Color Gamut Measurements and Mapping: The Role of Color Spaces", Proceedings of SPIE Electronic Imaging Conference, Vol. 3648, pp. 68-82.

Morovic J.
1998 "To Develop a Universal Gamut Mapping Algorithm", Ph.D. Thesis, University of Derby.

Montag E. D. and Fairchild M. D.
1997 "Psychophysical Evaluation of Gamut Mapping Techniques Using Simple Rendered Images and Artificial Gamut Boundaries", IEEE Trans. Image Processing., Vol. 6, pp. 977–989.

Montag E. D. and Fairchild M.D.
1998 "Gamut Mapping: Evaluation of Chroma Clipping Techniques for Three Destination Gamuts", Proceedings of the 6th IS&T/SID Color Imaging Conference, pp. 57-61.

Morovic J. and Luo M. R.
1997 "Gamut Mapping Algorithms Based on Psychophysical Experiment", Proceedings of the 5th IS&T/SID Color Imaging Conference, pp. 44–49.

Morovic J. and Luo M. R.
1998 "Verification Of Gamut Mapping Algorithms In CIECAM97s Using Various Printed Media", Proceedings of the 6th IS&T/SID Color Imaging Conference, pp. 53-56.

Stone M.C. and Wallace W.E.
1991 "Gamut Mapping Computer Generated Imagery", Graphics Interface '91, pp. 32-39.

Torgerson W.S.
1958 "Theory and Methods of Scaling" (John Wiley and Sons, Inc.)

Viggiano J.A.S and Wang J.
1992 "A Comparison of Algorithms for Color Matching Between Media of Differing Luminance Ranges", TAGA Proceedings, Vol. 2, pp. 959-974.

Wolski M., Allebach J. P. and Bouman C. A.
1994 "Gamut Mapping. Squeezing the Most out of Your Color System", Proceedings of the 2nd IS&T/SID Color Imaging Conference, pp. 89–92

Appendix A - Image-gamut calculation

1. Convert the CIELAB image data into CIELAB LCh coordinates.

2. Sort the image data into the nearest integer hue angle between 0 and 360 degrees.

3. For each hue angle convert the L* and the C_{ab}* values for the current hue and those of the two neighboring hue angles into polar coordinates about the cusp-point (L_{cusp}*) of the current hue center. This results in radius (ρ) and angle (α) terms, for each point, given respectively by:

$$\rho = \sqrt{\left(L^* - L^*_{cusp}\right)^2 + \left(C^*_{ab}\right)^2} \qquad \text{(A-1)}$$

$$\alpha = \tan^{-1}\left(\frac{L^* - L^*_{cusp}}{C^*_{ab}}\right) * \frac{180^\circ}{\pi} + 90^\circ \qquad \text{(A-2)}$$

4. Calculate the 2-dimensionial [ρ, α] histogram of the pixels in that hue and the two adjacent hue angles. The bin sizes used in the histogram calculation are [$\Delta\rho$,$\Delta\alpha$] = [1,1]. The two adjacent hue angle bins are used in the histogram process to insure smoothness between the hue segments around the hue circle. The gives a 181xN matrix of histogram values where the rows of the matrix are the α values from [0,180] degrees in 1 degree steps. The N columns of the matrix are in distance units from the cusp-point and cover the range of [0, k] where k = nearest integer of max(ρ) and N = k+1.

5. Calculate the cumulative histogram for each α by taking the cumulative sum along the rows of the [ρ, α] histogram.

6. Normalize each row of the cumulative histogram by dividing by the maximum value in each row.

7. For each row of the normalized cumulative histogram, determine the column (ρ) where the cumulative histogram equals (0.95). This radius is used to represent the image gamut for the current hue angle and the current angular deviation from the cusp point. This process results in a 181-term vector that represents the image gamut for the current hue angle.